Human Reproduction, pp. 1–14, 2022
https://doi.org/10.1093/humrep/deac237

human reproduction

ORIGINAL ARTICLE *Reproductive biology*

Role of apoptosis and autophagy in ovarian follicle pool decline in children and women diagnosed with benign or malignant extra-ovarian conditions

L. Cacciottola [1,†], A. Camboni[1,2,†], A. Cernogoraz[1,3], J. Donnez[4,5], and M.M. Dolmans [1,6,*]

[1]Gynecology Research Unit, Institut de Recherche Expérimentale et Clinique, Université Catholique de Louvain, Brussels, Belgium [2]Department of Anatomopathology, Cliniques Universitaires Saint-Luc, Brussels, Belgium [3]Department of Gynecology and Obstetrics, F. Del Ponte Hospital, University of Insubria, Varese, Italy [4]Society for Research into Infertility, Brussels, Belgium [5]Professor EM, Université Catholique de Louvain, Brussels, Belgium [6]Department of Gynecology, Cliniques Universitaires Saint-Luc, Brussels, Belgium

*Correspondence address. Gynecology Research Unit, Institut de Recherche Expérimentale et Clinique, Université Catholique de Louvain, Avenue Mounier 52, bte B1.52.02, 1200 Brussels, Belgium. Tel: +32-2-764-5237; Fax: +32-2-764-9507; E-mail: marie-madeleine.dolmans@uclouvain.be
https://orcid.org/0000-0002-6331-3026

Submitted on March 23, 2022; resubmitted on September 26, 2022; editorial decision on October 14, 2022

STUDY QUESTION: Which biological mechanisms are responsible for physiological ovarian reserve decline owing to aging, or pathological follicle depletion triggered by inflammation or a pro-oxidant environment throughout a woman's lifetime?

SUMMARY ANSWER: Ovarian follicle pool size is modulated by both apoptosis and autophagy, the first responsible for its physiological decline over time and increasing in the event of prior chemotherapy in children, and the latter playing a major role in physiological ovarian follicle pool diminution before puberty.

WHAT IS KNOWN ALREADY: Among the different pathways of controlled cell death, apoptosis and autophagy are implicated in follicle loss. Apoptosis participates in eliminating damaged follicles, such as those impaired by chemotherapy (CHT), but its involvement in physiological age-related follicle decline is less well understood. Autophagy has proved crucial in follicle quiescence maintenance in murine models, but its contribution to human follicle pool modulation is still unclear.

STUDY DESIGN, SIZE, DURATION: This retrospective study included 84 patients with benign or malignant extra-ovarian conditions aged between 1 and 35 years, with ovarian tissue stored for histological analyses at the time of cryopreservation (between 2012 and 2021) at a tertiary care center.

PARTICIPANTS/MATERIALS, SETTING, METHODS: Ovarian fragments were used for the following analyses: hematoxylin and eosin staining for follicle count and classification; cleaved caspase-3 immunostaining to identify follicle apoptosis; and microtubule-associated proteins 1A/1B light chain 3B immunolabeling to detect follicle autophagy. Transmission electron microscopy was also carried out to investigate ultrastructural features of oocytes and granulosa cells. All analyses stratified patients by age, menarchal status (premenarchal = 32; postmenarchal = 52), potentially gonadotoxic CHT before cryopreservation (n = 14), presence of endometriosis and use of hormonal treatment.

MAIN RESULTS AND THE ROLE OF CHANCE: Premenarchal patients had a larger follicle pool in terms of total follicle density [mean, range 4979.98 (342.2–21789) versus 918.8 (26.18–3983), $P < 0.001$], but higher rates of morphologically abnormal [8.52 (0–25.37)% versus 3.54 (0–17.5)%, $P < 0.001$] and atretic [15.8 (0–31.85)% versus 10.6 (0–33.33)%, $P < 0.01$] follicles than postmenarchal subjects. Apoptosis rates did not change with increasing age [27.94 (0–93.2)% in prepubertal subjects and 29.5 (0–100)% in postpubertal subjects], but autophagic follicles were around 10 times more common in premenarchal than postmenarchal subjects [10.21 (0–62.3)% versus 1.34 (0–25)%, $P < 0.001$], playing a crucial role in age-related follicle decline and elimination of 'abnormal' follicles, that are rarely seen after menarche. The impact of diagnosis and previous CHT varied according to age. In premenarchal patients with previous CHT, significantly more apoptotic [40.22 (0–100)% versus 26.79 (0–87)%, $P < 0.05$] and fewer abnormal [3.84 (0–10–76)% versus 9.83 (0–25.37)%, $P < 0.01$] follicles were detected than in subjects with no CHT prior to ovarian tissue cryopreservation, suggesting a direct

[†]These authors are co-first authors.

effect on follicle elimination, especially of those with abnormalities. In postmenarchal subjects with previous CHT, quiescent follicle rates were lower than in patients with no CHT before tissue freezing [71.57 (0–100)% versus 85.89 (50–100)%, $P < 0.05$], suggesting accelerated follicle activation and growth. Moreover, increased autophagic activity was observed in the event of a cancer diagnosis compared to benign conditions after puberty [26.27 (0–100)% versus 9.48 (0–29.41)%, respectively, $P < 0.05$].

LIMITATIONS, REASONS FOR CAUTION: The impact of specific CHT protocols could not be investigated since the group of patients with previous CHT was highly heterogeneous.

WIDER IMPLICATIONS OF THE FINDINGS: This study yields a deeper understanding of regulation of the follicle pool decline, showing for the first time that both apoptosis and autophagy pathways are involved in physiological follicle depletion, the latter being crucial before puberty. Moreover, our data showed a different response to non-physiological damage according to age, with higher apoptosis rates only in premenarchal subjects with previous CHT, confirming that this pathway is activated by drugs known to induce DNA damage in oocytes, such as alkylating agents, but not by cancer itself.

STUDY FUNDING/COMPETING INTEREST(S): This study was supported by grants from the Fonds National de la Recherche Scientifique de Belgique (F.R.S.-FNRS/FRIA FC29657 awarded to L.C., CDR J.0063.20 and grant 5/4/150/5 awarded to M.M.D.), grants from the Fondation contre le Cancer (grant 2018-042 awarded to A.Ca.), the Fondazione Comunitaria del Varesotto and Provincia di Varese ('Amalia Griffini' Fellowship in Gynecology and Obstetrics awarded to A.Ce.), Fonds Spéciaux de Recherche, Fondation St Luc and donations from the Ferrero family. The authors have no competing interests to declare.

TRIAL REGISTRAION NUMBER: N/A.

Key words: ovarian reserve / fertility preservation / prepubertal ovaries / follicle atresia / apoptosis / autophagy / chemotherapy / follicle activation / ovarian damage

Introduction

The number of follicles in the ovary is determined during embryonic life. At around 18–22 weeks of gestational age, it reaches a peak of 6 million and then starts its inevitable decline, dropping to ~1000 follicles by the end of the reproductive lifespan, resulting in menopause (Wallace and Kelsey, 2010). The main factor responsible for follicle loss over the years is follicle atresia, which occurs in both growing and non-growing follicles (Gougeon and Chainy, 1987). Follicle atresia has been widely documented as histological evidence of ongoing cell death. It is characterized by: nuclear pyknosis and cytoplasmic condensation in granulosa cell (GC) layers; irregular follicle and/or oocyte shape; reduced total cell volume; and a related increase in cell density (Gougeon, 1996). However, physiological regulation of this phenomenon and the signaling pathways sustaining its continuous activity remain somewhat elusive. More recently, different pathways of controlled cell death occurring through signaling pathway activation and requiring energy use have been reported to be involved in age-related follicle pool decline, namely follicle apoptosis (Tilly, 2001; Tiwari *et al.*, 2015) and autophagy (Yadav *et al.*, 2019; Zhou *et al.*, 2019).

Apoptosis is a cell death mechanism involved in fetal formation and regulation of the ovarian reserve (Hartley *et al.*, 2002; Albamonte *et al.*, 2008). After birth, it is responsible for eliminating damaged oocytes to ensure the development of those of good quality (Vaskivuo and Tapanainen, 2003; Yadav *et al.*, 2019). Impaired oocyte quality can result from increased levels of oxidative stress caused by either physiological conditions such as aging or pathological triggers causing inflammation and a pro-oxidant environment (Tiwari *et al.*, 2017; Yadav *et al.*, 2019). Oxidative stress may potentially damage DNA, which is of vital importance in oocytes for genome preservation and transmission to offspring. Indeed, oocytes have dedicated pathways to deal with DNA impairment through activation of the apoptosis cascade (Tilly, 2001; Ellnati *et al.*, 2020; Maidarti *et al.*, 2020). Caspase-3 activation by cleavage of its inactive zymogen (procaspase-3) triggers DNA cleavage by caspase-dependent DNase, resulting in nuclear fragmentation and cell death (Hurst *et al.*, 2006). Apoptosis generated by caspase-3 appears to be implicated in follicle depletion consequent to chemotherapy (CHT) (Spears *et al.*, 2019; Luan *et al.*, 2019; Nguyen *et al.*, 2021; Dolmans *et al.*, 2021a; Cacciottola *et al.*, 2021a) and hypoxia induced by ovarian tissue transplantation (Dolmans *et al.*, 2007, 2021a; Cacciottola *et al.*, 2021), emphasizing its role in eliminating damaged follicles.

Autophagy is a complex cell mechanism whereby cells disassemble and recycle dysfunctional cellular components for either adaptive survival responses or induction of cell death and follicle atresia (Gawriluk *et al.*, 2011; Rubinsztein *et al.*, 2011). A number of pathways are believed to participate in regulating autophagy, but many regulatory mechanisms are still poorly understood. To date, 5′-AMP-activated protein kinase (AMPK) and mammalian target of rapamycin (mTOR) pathways are believed to be the major pathway regulators (Zhou *et al.*, 2019). Autophagy has various catalysts, such as starvation, hypoxia or hormonal stimulation, which cause upregulation of AMPK or inhibition of mTOR. This results in the formation of double-membrane vacuoles, called autophagosomes, by the activation of beclin 1 and class III phosphoinositide 3-kinase, and also downstream autophagy components such as microtubule-associated proteins 1A/1B light chain 3B (LC3B). Activated LC3B then inhabits autophagosome surfaces and plays a key role in the final stages of autophagy, like lysosome fusion for content degradation (Duerrschmidt *et al.*, 2006; Zhou *et al.*, 2019).

In the context of the ovary, autophagy is considered crucial to maintenance of the follicle pool throughout reproductive life, playing a specific role in follicle survival before puberty (Gawriluk *et al.*, 2011; Song *et al.*, 2015) and maturation during a woman's fertile lifespan (Escobar *et al.*, 2019). Knockout mice for autophagy-related (ATG) proteins 5 or 7, which are essential components for formation of autophagosomes, experience germ cell loss soon after birth and show an altered morphology and distribution of remaining follicles, with elevated follicle atresia rates, ultimately inducing

premature ovarian failure (Gawriluk *et al.*, 2011; Song *et al.*, 2015). Moreover, impaired autophagy, namely reduced formation and elimination of autophagosomes, may play a role in ovarian aging and hence diminish oocyte quality (Peters *et al.*, 2021).

Previous studies on murine models identified crosstalk between autophagy and apoptosis through the autophagy-mediated activation of proapoptotic signals, leading to follicle death (Choi *et al.*, 2011; Escobar *et al.*, 2019). The majority of these mechanisms were detected in murine ovaries, but we still lack information on the human follicle pool. The aim of our study was therefore to gain further insights into patterns of follicle loss kinetics in different conditions, including age (childhood, adolescence and childbearing age) and after CHT, to enhance our understanding of the underlying mechanisms and ultrastructural modifications.

Materials and methods

Subjects

Human ovarian tissue fragments fixed for histological analyses at the time of ovarian tissue cryopreservation (OTC) between 2012 and 2021 were collected from the biobank of the Université Catholique de Louvain (UCL), after obtaining approval from the Institutional Review Board (UCL, 2012/23MAR/125). Based on this approval and tissue sample availability, a total of 92 subjects were selected. Patients undergoing OTC for Turner syndrome (n = 3) or benign or malignant ovarian pathologies such as endometriomas or ovarian cancer (n = 2), and those showing evidence of metastasis in their residual ovarian tissue (n = 3), were excluded. The remaining 84 subjects were included in the present study.

Indications for fertility preservation were benign conditions in 12 patients (14.29%), and cancer diagnoses in the remaining 72 (85.71%) (Fig. 1A). Patient age ranged from 1 to 35 years. Thirty-two subjects (38.09%) had had their ovarian tissue cryopreserved before menarche, at an average age of 6.28 ± 3.68 years, while the mean age of postmenarchal subjects was 23.6 ± 7.17 (Fig. 1B). Among the 52 postmenarchal patients, 24 were under hormone treatment at the time of OTC. In six patients, three of whom were taking hormones and three of whom were not, peritoneal endometriosis was identified during laparoscopy for OTC (Fig. 1B). A total of 14 patients had undergone a combined CHT regimen, including alkylating agents, platinum and/or anthracycline prior to OTC. Two of them had had CHT around 2 and 4 years before and had their ovarian tissue frozen at the time of recurrence, before a second CHT treatment (Supplementary Table SI).

Histology

Ovarian fragments were fixed in 4% formaldehyde immediately after surgery and then included in paraffin blocks for long-term storage in the Department of Anatomopathology at the Cliniques Universitaires Saint-Luc. As antigenicity is preserved in paraffin blocks for long periods of time and its decay only begins after 15–20 years, only blocks up to 10 years old were selected for the study (Grillo *et al.*, 2017). Five-micrometer sections were obtained for each block to perform histological and immunohistochemical staining on stored ovarian cortex. After staining, all slides were digitized using the Pannoramic P250 Flash III scanner (3DHistech, Budapest, Hungary) and analyzed by CaseViewer v2.3 (3DHistech, Budapest, Hungary).

Follicle count and classification

Up to three nonconsecutive sections from each sample were stained with hematoxylin and eosin (Merck, Darmstadt, Germany) and investigated. Follicle density was determined by counting the number of follicles with a visible oocyte per mm^3 on digitized slides. Volume was calculated by multiplying digitized surfaces by fragment thickness. Follicles were then counted and categorized according to their developmental stage. Normal-looking follicles were classified as: quiescent, namely primordial with a single layer of flattened GCs surrounding the oocyte, or intermediate, with one layer of both flattened and cuboidal GCs; or growing, namely primary with a complete layer of cuboidal GCs around the oocyte, secondary, with two or more layers of cuboidal GCs, or antral, when a cavity was detected within the GC layers (Gougeon and Chainy, 1987). Follicle atresia was evaluated using strict morphological criteria, including ooplasm eosinophilia, GC pyknosis, cytoplasmic contraction and the presence of vacuoles (Gougeon and Chainy, 1987). Abnormal follicles were divided into three subcategories: double, if they accommodated two nuclei or two oocytes in the same GC layer; vacuolized, if vacuoles were clearly observed in GCs or the oocyte cytoplasm without signs of atresia; and asymmetric, if the GC layer consisted of multiple cell layers in just one spot or was incomplete (Sadeu *et al.*, 2006; Mamsen *et al.*, 2019).

Follicle apoptosis

Up to three nonconsecutive sections from each sample were allocated to immunolabeling for cleaved caspase-3 (c-caspase-3) as a marker of apoptosis. Embedded sections were first deparaffinized, then rehydrated in 2-propanol (Merck, Darmstadt, Germany) and demineralized water. Endogenous peroxidase activity was inhibited by incubating the sections in 3% H_2O_2 for 30 min at room temperature. They were then decloaked in citrate buffer (pH 6) for 75 min in a 98°C water bath, before incubation in normal goat serum and bovine serum albumin to block nonspecific binding sites for 30 min at room temperature. The sections were incubated overnight at 4°C with the primary antibody, rabbit anti-human c-caspase-3 (1:200, 9661S; Cell Signaling Technology, Danvers, MA, USA), before another 60 min at room temperature with EnVision rabbit horseradish peroxidase (HRP) (1:1, K4003, Dako, Sant Clara, CA, USA). Diaminobenzidine (DAB) (substrate kit, Vector Laboratories, Newark, CA, USA) was used as a chromogen. Human tonsil tissue served as positive controls, while negative controls were obtained using nonspecific rabbit antibodies on human ovarian tissue fragments (Cacciottola *et al.*, 2021). Digitized slides were then analyzed, with follicles classified as apoptotic when either the oocyte or >50% of GCs, or indeed both, were positive (Amorim *et al.*, 2019). Apoptosis rates were assessed by counting positive follicles out of total analyzed follicles as a percentage.

Follicle autophagy

Up to three nonconsecutive sections from each sample were assigned to immunolabeling for LC3B, a marker of autophagy. Embedded sections were deparaffinized before rehydratation in 2-propanol (Merck, Darmstadt, Germany) and demineralized water. Endogenous peroxidase

A

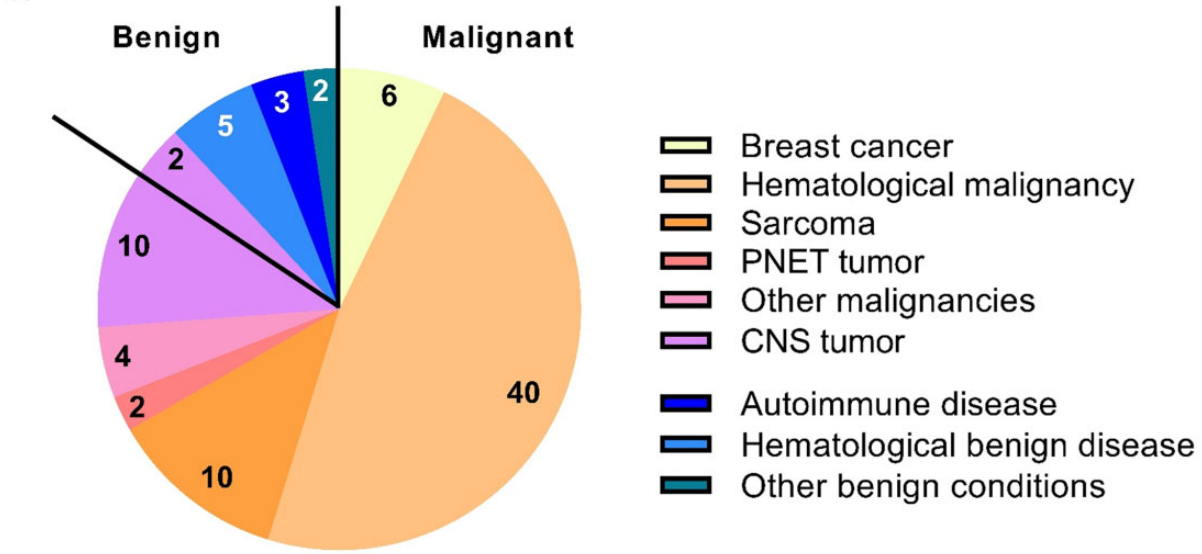

B

Patient characteristics	Premenarche	Postmenarche		Total
Menarchal status	32/84 (38.09%)	52/84 (61.11%)		84
Age	6.28 ± 3.68**	23.6 ± 7.17**	*p<0.01*	17 ± 10.1
Hormonal treatment	/	24/52 (46.15%)		24/52 (46.15%)
Evidence of endometriosis	/	6/52 (11.53%)		6/52 (11.53%)
Indication for fertility preservation				
Cancer diagnosis	25/32 (78.1%)	47/52 (90.38%)	*ns*	72/84 (85.71%)
Benign condition	7/32 (21.9%)	5/52 (9.62%)	*ns*	12/84 (14.29%)
Previous CHT	7/32 (21.8%)	7/52 (13.4%)	*ns*	14/84 (16.66%)

Figure 1. Patient characteristics. (**A**) Distribution of patients requiring fertility preservation by diagnosis, with each section showing the number of patients with the same diagnosis, specified in the list on the right side of the graph. Black lines denote subgroups of 12 patients with benign conditions and 72 patients with a cancer diagnosis. (**B**) Description of patient characteristics according to their menarchal status. CHT, chemotherapy; CNS, central nervous system; PNET, primitive neuroectodermic tumor.

activity was inhibited by incubating the slides in 3% H_2O_2 for 30 min at room temperature. Decloaking was carried out in citrate buffer (pH 6) for 75 min in a 98°C water bath. The sections were incubated in normal goat serum, bovine serum albumin and 2% nonfat milk solution and then overnight at 4°C with the primary antibody, rabbit anti-human LC3B (1:1000, 3868S; Cell Signaling Technology). The slides were subsequently incubated for 60 min at room temperature with EnVision HRP (1:1, K4003, Dako, Sant Clara, CA, USA), and DAB (substrate kit, Vector Laboratories, Newark, CA, USA) was used as a chromogen. Human adrenal gland tissue served as positive controls, while negative controls were obtained using nonspecific rabbit antibodies on human ovarian fragments (Cacciottola *et al.*, 2021). Digitized slides were analyzed as follows. Follicles were considered positive when either the oocyte or GCs, or both, were stained. Positive follicles were then divided into two groups based on semiquantitative criteria: follicles with individual positive spots representing autophagosomes in oocytes as a sign of physiological cell renewal through autophagic activity; and follicles with multiple and merging spots representing extensive presence of autophagosomes, potentially triggering autophagic cell death (Peters *et al.*, 2021). Autophagic follicle rates were evaluated by counting positive follicles out of total analyzed follicles as a percentage.

Transmission electron microscopy

For ultrastructural analysis, small ovarian tissue fragments from 13 patients (two premenarchal, seven postmenarchal and four postmenarchal with prior CHT) were fixed in 2.5% glutaraldehyde for 48 h. After fixation, the samples were washed in PBS solution and postfixed in 1% osmium tetroxide for 2 h. They were rinsed and dehydrated through an ascending series of ethanol, before being embedded in epoxy resin (Agar Scientific, Essex, UK). The resin blocks were sectioned using an Ultracut E ultramicrotome (Reichert technologies, Depew, NY, USA), and semithin sections (3-µm thick) were stained with

toluidine blue and inspected by light microscopy. Ultrathin sections (60–90 nm) were then acquired using a diamond knife, mounted on copper grids and contrasted with saturated uranyl acetate and lead citrate. They were examined and photographed with a Zeiss EM10 electron microscope operating at 80 kV (Zeiss, Oberkochen, Germany). Transmission electron microscopy (TEM) analyzed and revealed the ultrastructural characteristics of GCs and oocytes, as well as their plasma membranes, nuclear envelope and organelles (Nottola *et al.*, 2006; Camboni *et al.*, 2008). Follicles with: a continuous layer of GCs; preserved junctions between GCs and the oocyte; no evidence of organelle swelling or abnormal distribution; and good-quality chromatin were considered healthy. Particular emphasis was placed on cytoplasmic autophagosomes, which were counted on every section. As previously done for LC3B staining, semiquantitative analysis was performed. Follicles showing 1–3 autophagosomes per section were assumed to be exhibiting some autophagic activity, while those with more than three autophagosomes per section were considered to be undergoing autophagic cell death (Martinet *et al.*, 2014; Klionsky *et al.*, 2021).

Statistical analysis

Ordinary least square multiple regressions were performed using RStudio (Boston, MA, USA). Age and previous CHT were independent variables for the whole population (n = 84), while the presence of endometriosis and use of hormonal treatment were used as independent variables only for the subgroup of postmenarchal patients (n = 52). Data on follicle densities were transformed to logarithmic scale for analyses. Results are presented as estimates, with their SEs and CIs. Statistical analyses for further subgroup comparisons were performed using Prisma GraphPad 9.2 (Dotmatics, San Diego, CA, USA). Student's *t*-test, the Mann–Whitney non-parametric test, or chi-square test, where appropriate, were used according to data normal distribution. Age was presented as mean ± SD, and all other results as mean (min–max). *P* values <0.05 were considered statistically significant.

Results

The characteristics of patients whose tissues were analyzed are shown in Fig. 1.

Impact of age on the ovarian reserve

Linear regression was conducted to assess the relation between patient characteristics and different follicle outcomes. A negative correlation was found between age and follicle density (Table I). More specifically, all follicle populations (normal-looking, abnormal and atretic) declined significantly with advancing age (Fig. 2A–C). Follicle outcomes according to menarchal status are reported in Table II as follicle densities (#/mm^3) and rates (# follicles per subgroup as a percentage). Mean follicle density was significantly higher in premenarchal compared to postmenarchal patients ($P < 0.001$). Follicle morphology, however, showed lower rates of normal-looking follicles in premenarchal subjects than in postmenarchal women ($P < 0.001$), although their absolute number was significantly higher ($P < 0.001$). Abnormal follicles accounted for a significantly greater share in premenarchal patients in terms of both density ($P < 0.001$) and rates of total follicles ($P < 0.001$). Atretic follicles exhibited the same pattern, with significantly higher density ($P < 0.001$) and rates ($P < 0.05$) in premenarchal subjects (Table II). Quiescent follicle (primordial and intermediate) rates were significantly higher in premenarchal than postmenarchal patients ($P < 0.05$), representing the largest proportion of normal-looking follicles in both groups.

Mechanisms of follicle death and menarchal status

Linear regression was used to evaluate the correlation between patient characteristics and follicle death mechanisms (Table III). The results showed an inverse correlation between age and autophagic follicle death, the latter decreasing with increasing age (Fig. 3A–C). Apoptosis and autophagy activation rates were similar in premenarchal and postmenarchal subjects, while autophagic death rates were significantly higher in premenarchal than postmenarchal subjects [10.21 (0–62.3)% versus 1.34 (0–25)%, $P < 0.001$] (Table II).

Hormonal treatment and presence of endometriosis in postmenarchal patients

In postpubertal patients, linear regression applied to patient characteristics, such as hormone treatment and presence of peritoneal endometriosis, found no correlation with different follicle populations (Table I) or follicle death mechanisms (apoptosis, autophagy activation, autophagic death) (Table III).

Impact of cancer diagnosis and previous CHT on follicle kinetics

Three patient groups were taken into account for both premenarchal and postmenarchal groups: subjects with benign conditions; subjects with malignancies; and subjects who had undergone some CHT with alkylating agents prior to OTC. Among premenarchal patients, 6 were diagnosed with benign conditions, 19 with malignancies and 7 had had some previous CHT (Table IV). No difference was noted in total, normal-looking or atretic follicle density between groups. However, abnormal follicle rates were significantly lower in case of previous CHT compared to no CHT before OTC [3.84 (0–10–76)% versus 9.83 (0–25.37)%, $P < 0.05$]. There was no difference in quiescent follicle rates between groups. With respect to follicle death mechanisms, higher apoptosis rates were encountered in patients with previous CHT [40.22 (0–100)% versus 26.79 (0–87)%, $P < 0.05$], while no difference was evidenced in autophagy activation rates or autophagic follicle death rates.

Among postmenarchal patients, 5 were diagnosed with benign conditions, 40 with malignancies and 7 had had some previous CHT (Table V). Total, normal-looking, abnormal and atretic follicle density was similar between groups. Regarding follicle quiescence and growth, subjects with prior CHT exhibited lower rates of quiescent follicles [71.57 (0–100)% versus 85.89 (50–100)%, $P < 0.05$] compared to those without any CHT. Patients diagnosed with malignancies showed more autophagy activation than those with benign conditions [26.27 (0–100)% versus 9.48 (0–29.41)%, $P < 0.05$], while there was no difference compared to those with some previous CHT.

Table I Linear regression between independent* and dependent† variables.

	Follicle density†		Normal-looking follicle density†		Abnormal follicle density†		Atretic follicle density†	
	Coefficient (SE)	CI	Coefficient (SE)	CI	Coefficient (SE)	CI	Coefficient (SE)	CI
(Intercept)	*8.599*** *(0.216)*	*(8.176, 9.023)*	*8.225*** *(0.216)*	*(7.801, 8.649)*	*6.410*** *(0.405)*	*(5.616, 7.204)*	*6.931*** *(0.420)*	*(6.108, 7.754)*
*Age	−0.095** (0.011)	(−0.116, −0.074)	−0.086** (0.011)	(−0.107, −0.066)	−0.181** (0.020)	(−0.220, −0.142)	−0.151** (0.020)	(−0.191, −0.111)
*Previous CHT	0.036 (0.284)	(−0.521, 0.593)	0.119 (0.284)	(−0.438, 0.676)	−1.052 (0.532)	(−2.095, −0.008)	−0.471 (0.552)	(−1.553, 0.610)
Observations	*84*		*84*		*84*		*84*	
R^2	*0.503*		*0.457*		*0.514*		*0.402*	
Adj. R^2	*0.49*		*0.443*		*0.502*		*0.387*	
(Intercept)	*8.058*** *(0.547)*	*(6.985, 9.130)*	*7.681*** *(0.539)*	*(6.625, 8.737)*	*6.485*** *(0.961)*	*(4.602, 8.367)*	*6.853*** *(1.081)*	*(4.734, 8.972)*
*Endometriosis	−0.458 (0.440)	(−1.321, 0.405)	−0.439 (0.433)	(−1.289, 0.411)	0.581 (0.760)	(−0.895, 2.135)	−1.402 (0.870)	(−3.108, 0.303)
*Hormonal treatment	0.378 (0.297)	(−0.205, 0.961)	0.334 (0.293)	(−0.240, 0.908)	−0.098 (0.522)	(−1.121, 0.926)	0.963 (0.588)	(−0.189, 2.115)
Observations	*52*		*52*		*52*		*52*	
R^2	*0.228*		*0.191*		*0.354*		*0.259*	
Adj. R^2	*0.162*		*0.122*		*0.299*		*0.196*	

Coefficient estimates are from Ordinary Least Squares. Standard errors (SE) are in parentheses. CHT, chemotherapy.
**$P < 0.01$.

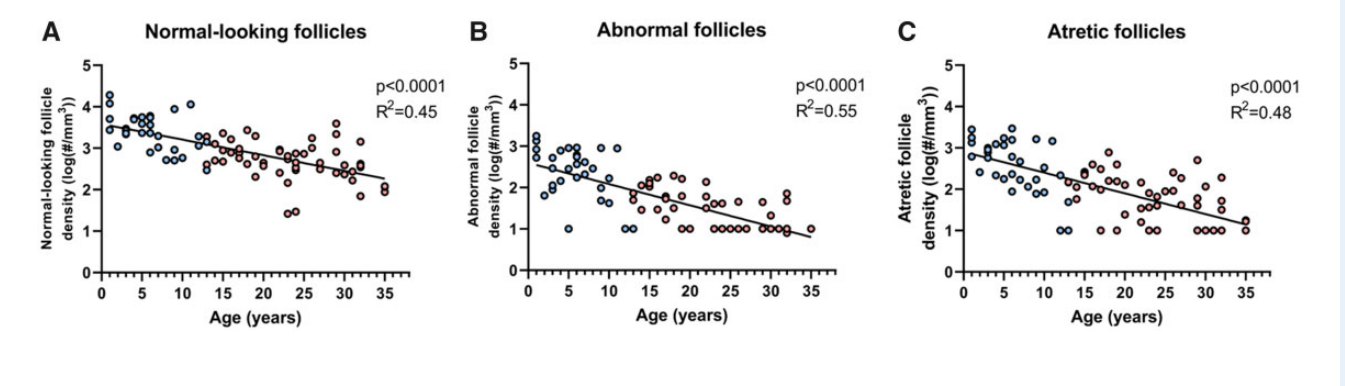

Figure 2. Correlation between age and density of normal, abnormal and atretic follicles. Correlation between age and follicle density of (**A**) normal-looking, (**B**) abnormal and (**C**) atretic follicles.

Abnormal follicle populations

Further analysis of specific subtypes of morphological anomalies, namely double, vacuolized and asymmetric (Fig. 4A–C), revealed a positive correlation between total follicle density and abnormal follicle proportions, irrespective of age ($P = 0.04$) (Fig. 4D). Moreover, postmenarchal subjects showed significantly smaller proportions of double and asymmetric follicles than did premenarchal subjects (Fig. 4E).

Follicle ultrastructure

A total of 116 preantral follicles (primordial or primary) were analyzed, including 30 from premenarchal patients (n = 1), 53 from postmenarchal patients (n = 7) and 33 from postmenarchal patients who had received some CHT prior to OTC (n = 4). Statistical comparisons between groups did not consider premenarchal patients, since only one patient was involved. Healthy follicle rates were 53% in premenarchal subjects (16/30), 71% in

Table II Follicle outcomes in premenarchal and postmenarchal subjects.

Follicle parameters	Premenarche	Postmenarche	
Total follicle density	4979.98 (342.2–21789)***	918.8 (26.18–3983)***	*P < 0.001*
Normal-looking follicle density	3790.52 (293.5–19113)***	768.17 (26.18–3922)***	*P < 0.001*
% out of total	75.66 (53.84–100)***	85.82 (55–100)***	*P = 0.001*
Abnormal follicle density	417.05 (0–1775)***	38.07 (0–193.1)***	*P < 0.001*
% out of total	8.52 (0–25.37)***	3.54 (0–17.5)***	*P < 0.001*
Atretic follicle density	772.4 (0–2950)***	112.4 (0–772.5)***	*P < 0.001*
% out of total	15.8 (0–31.85)*	10.67 (0–33.33)*	*P < 0.05*
Follicle classification			
Quiescent follicles (%)	92.45 (66.67–100)*	84.29 (0–100)*	*P < 0.05*
Growing follicles (%)	7.54 (0–33.32)	15.70 (0–100)	/
Follicle apoptosis (%)	27.94 (0–93.2)	29.5 (0–100)	*ns*
Autophagy activation (%)	22.93 (0–100)	23.24 (0–100)	*ns*
Autophagic follicle death (%)	10.21 (0–62.3)***	1.34 (0–25)***	*P < 0.001*

Values are expressed as mean (min–max). ns, not significant.
*$P < 0.05$.
**$P < 0.01$.
***$P < 0.001$.

Table III Linear regression between independent* and dependent† variables.

	Follicle apoptosis†		Autophagy activation†		Autophagic follicle death†	
	Coefficient (SE)	**CI**	**Coefficient (SE)**	**CI**	**Coefficient (SE)**	**CI**
(Intercept)	*26.523** (7.361)*	*(12.096, 40.951)*	*21.558** (4.577)*	*(12.587, 30.529)*	*9.081** (2.507)*	*(4.167, 13.996)*
***Age**	0.182 (0.358)	(−0.519, 0.884)	0.140 (0.223)	(−0.296, 0.576)	−0.273* (0.122)	(−0.512, −0.034)
***Previous CHT**	5.890 (9.650)	(−13.024, 24.805)	−4741 (6.001)	(−16.502, 7.020)	2.109 (3.287)	(−4.334, 8.552)
Observations	*82*		*82*		*82*	
R^2	*0.007*		*0.014*		*0.067*	
Adj. R^2	*−0.018*		*−0.011*		*0.044*	
(Intercept)	*13.312 (19.503)*	*(−24.914, 51.538)*	*17.516 (11.352)*	*(−4.732, 39.765)*	*−2.562 (2.188)*	*(−6.851, 1.728)*
***Endometriosis**	0.635 (16.694)	(−32.084, 33.354)	−7101 (9.716)	(−26.145, 11.943)	−1.348 (1.873)	(−5.020, 2.323)
***Hormonal treatment**	−2.943 (10.630)	(−24.914, 51.538)	−4.756 (6.187)	(−4.732, 39.765)	−2.562 (2.188)	(−6.851, 1.728)
Observations	*50*		*50*		*50*	
R^2	*0.024*		*0.057*		*0.112*	
Adj. R^2	*−0.063*		*−0.027*		*0.033*	

Coefficient estimates are from Ordinary Least Squares. Two patients were excluded as no follicles with normal morphology were found in immunohistochemistry slides for analyses. Standard errors (SE) are in parentheses. CHT, chemotherapy.
*$P < 0.05$.
**$P < 0.01$.

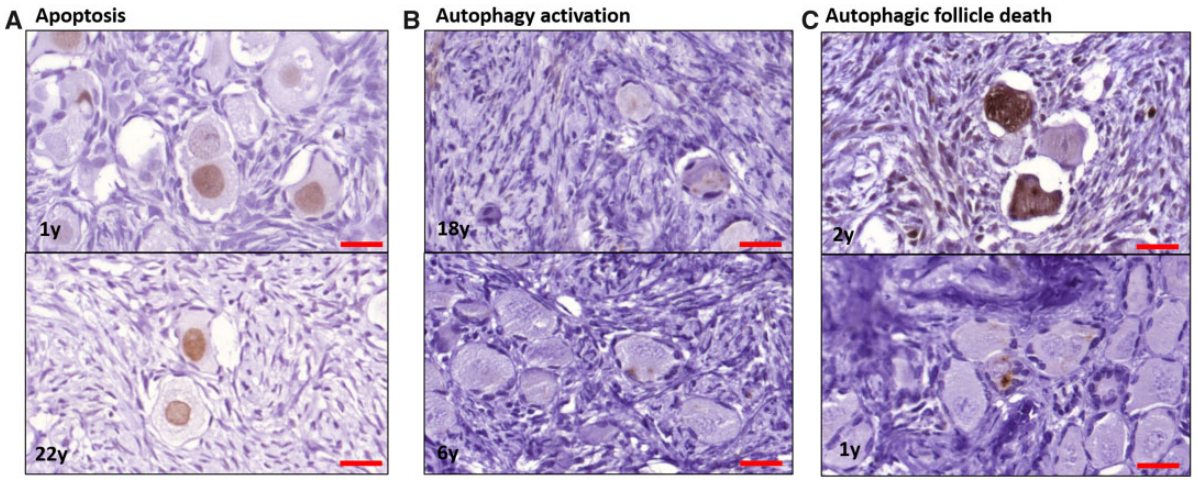

Figure 3. Immunolabeling for apoptosis, autophagy activation and autophagic follicle death before and after puberty. (**A**) Immunostaining for cleaved caspase-3 in oocytes from primordial and abnormal early-stage follicles in subjects aged 1 and 22 years (y), respectively. (**B**) Immunostaining for LC3B in oocytes from primordial follicles showing some positive spots, suggestive of autophagy activation owing to autophagosome formation, in subjects aged 18 and 6 years, respectively. (**C**) Immunostaining for LC3B in early-stage follicles revealing extended autophagic activity, leading to follicle death in subjects aged 2 and 1 years, respectively. Scale bar: 20 μm.

Table IV Impact of diagnosis and previous chemotherapy in premenarchal patients.

Premenarchal patients (32)	No previous CHT (25)			Previous CHT (7)	
	Benign conditions (6)	Malignancies (19)	Total (25)		
Age (± SD)	5.66 (2.33)	6.78 ± 4.13	6.52 ± 3.76	5.42 ± 3.5	*ns*
Total follicle density	3157.14 (1090–6494)	5602.54 (342.3–21789)	5015.64 (342.3–21789)	48522.62 (1425–7576)	*ns*
Normal-looking follicle density	2082.43 (915–3876)	4272.79 (293.5–19113)	3747.1 (293.5–19113)	3945.58 (1425–5595)	*ns*
% out of total	70.43 (59.7–83.92)	74.47 (53.84–100)	73.5 (53.84–100)	83.35 (68.97–100)	*ns*
Abnormal follicle density	360.16 (6.29–901.4)	500.02 (0–1775)	466.45 (0–1775)	240.62 (0–784.8)	*ns*
% out of total	9.98 (4.54–17.25)	9.78 (0–25.37) a	9.83 (0–25.37) a	3.84 (0–10–76) b	$P < 0.05$
Atretic follicle density	714.53 (77.87–1713)	829.72 (0–2950)	666.4 (0–2950)	802.08 (0–1557)	*ns*
% out of total	19.57 (7.14–30.84)	15.73 (0–31.85)	12.78 (0–31.85)	16.65 (0–27.59)	*ns*
Follicle classification					
Quiescent follicles (%)	92.72 (80.85–100)	90.92 (66.67–100)	96.36 (66.67–100)	91.35 (94.16–100)	*ns*
Growing follicles (%)	7.28 (0–19.15)	9.07 (0–32.33)	3.63 (0–32.33)	8.64 (0–5.90)	*ns*
Follicle death mechanisms					
Follicle apoptosis (%)	20.61 (0–40.3)	28.74 (0–87)	26.79 (0–87) a	40.22 (0–100) b	$P < 0.05$
Autophagy activation (%)	25.92 (2.77–44.68)	22.59 (0–100)	21.28 (0–100)	23.39 (0.76–46.15)	*ns*
Autophagic follicle death (%)	6.67 (0–20)	9.98 (0–45.24)	13.85 (0–45)	13.85 (0–62.5)	*ns*

Values are expressed as mean (min–max); statistically significant differences are indicated by different letters for every row (a ≠ b, $P < 0.05$). CHT, chemotherapy; ns, not significant.

postmenarchal subjects (28/53) and 85% in postmenarchal subjects with prior CHT (28/33) (Fig. 5A–D); no statistical differences were noted between the two latter groups. Autophagic death in follicles was observed only in premenarchal girls, in 8/30 follicles (26%) (Fig. 5E–F). Autophagic activity in follicles, on the other hand, was found in all groups, namely in 20/30 follicles (66%) in premenarchal subjects, 7/53 follicles (13%) in postmenarchal subjects and 2/33 follicles (6%) in postmenarchal subjects who had

Table V Impact of diagnosis and previous chemotherapy in premenarchal patients.

Postmenarchal patients (52)	No previous CHT (25)			Previous CHT (7)	
	Benign conditions (5)	Malignancies (40)	Total (45)		
Age	23.2 ± 7.36	23.37 ± 6.61	23.72 ± 6.51	25.14 ± 5.55	*ns*
Total follicle density	814.48 (470.1–1117)	931.71 (29.46–3693)	826.87 (29.46–3693)	919.54 (26.18–2983)	*ns*
Normal-looking follicle density	663.93 (417.8–966.3)	765.19 (29.46–2728)	681.55 ± (29.46–2728)	859.63 (26.18–3922)	*ns*
% out of total	81.93 (55–95.31)	85.64 (64.71–100)	85.45 (55–100)	88.78 (66.66–100)	*ns*
Abnormal follicle density	48.93 (0–151.3)	41.64 (0–193.1)	38.78 (0–193.1)	9.88 (0–31.78)	*ns*
% out of total	5.5 (0–17.5)	3.47 (0–15.4)	3.69 (0–17.5)	2.52 (0–10.53)	*ns*
Atretic follicle density	101.61 (40.17–197.6)	124.87 (0–772.5)	106.53 (0–772.5)	48.89 (0–117.6)	*ns*
% out of total	12.51 (4.69–27.5)	10.79 (0–29.47)	10.84 (0–29.47)	8.68 (0–33.33)	*ns*
Follicle classification					
Quiescent follicles (%)	86.26 (50–96.72)	85.78 (50–100)	85.89 (50–100) a	71.57 (0–100) b	$P < 0.05$
Growing follicles (%)	13.73 (3.37–50)	14.21 (0–50)	14.1 (0–50)	28.43 (0–100)	*ns*
Follicle death mechanisms					
Follicle apoptosis (%)	28.37 (6.08–84.21)	31.74 (0–100)	32.58 (0–100)	30.17 (0–100)	*ns*
Autophagy activation (%)	9.48 (0–29.41) a	26.27 (0–100) b	24.95 (0–100)	16.63 (0–35.29)	$P < 0.05$
Autophagic follicle death (%)	1.17 (0–5.88)	1.58 (0–25)	1.61 (0–25)	0.17 (0–1.19)	*ns*

Values are expressed as mean (min–max); statistically significant differences are indicated by different letters for every row (a ≠ b, $P < 0.05$). CHT, chemotherapy; ns, not significant.

undergone CHT prior to OTC; no statistical differences were observed between the two latter groups (Fig. 5G).

Discussion

The present study takes into account the two major mechanisms of controlled death that may be involved in follicle depletion, namely apoptosis and autophagy, by investigating a large cohort of ovarian tissue samples from children and young women. Our findings on follicle pool kinetics revealed a continuous decline in all follicle populations with advancing age, consistent with the literature (Wallace and Kelsey, 2010). In postpubertal subjects, use of hormonal treatment did not appear to affect the ovarian reserve in terms of follicle populations or death mechanisms. Similarly, the presence of peritoneal endometriosis did not seem to have any impact either. Robust literature points to a detrimental effect of endometriosis on the ovarian follicle pool (Kitajima *et al.*, 2014; Sanchez *et al.*, 2014), with this disease increasingly considered an indication for fertility preservation in its more aggressive clinical presentations (Dolmans and Donnez, 2021). Our findings may appear in contrast with this, but it is important to point out that none of our patients had symptomatic disease on their ovaries but, in all cases, only superficial peritoneal endometriotic lesions, which are less implicated in potential ovarian damage.

Special emphasis was placed on abnormal and atretic follicle populations, showing that they were more widely represented in younger patients. These results reveal a special role for both atretic and abnormal follicles in continuing mechanisms of depletion starting prior to birth and causing ovarian follicle pool decline in adulthood (Wallace and Kelsey, 2010; Luyckx *et al.*, 2013).

The two main mechanisms responsible for age-dependent ovarian reserve depletion are follicle recruitment and atresia (Gougeon, 1996). In our study, the premenarchal group had an average age of 6 years, significantly lower than when maximum non-growing follicle recruitment occurs, which is around 15 years (Wallace and Kelsey, 2010). Premenarchal subjects had significantly more quiescent follicles, confirming that follicle recruitment for further growth is not a notable cause of follicle depletion in this group. In ovaries from fetuses and prepubertal subjects, atresia is known to play a major role in follicle loss, estimated to reach 50% by the time of birth (Baker, 1963). Atretic follicle rates fall progressively with advancing age (Gougeon *et al.*, 1994; Vaskivuo and Tapanainen, 2003) and the start of follicle recruitment and growth, as a consequence of gonadal axis activity.

Follicle apoptosis is an energy-requiring process that leads to DNA fragmentation and cell shrinkage without membrane rupture (Vaskivuo and Tapanainen, 2003). The present study detected ongoing follicle apoptosis in fresh ovarian tissue, irrespective of ovarian damage, endocrine status or follicle pool size. Apoptosis can be triggered in both oocytes and GCs. In the literature, caspase-3-mediated apoptosis is commonly observed in GCs of antral follicles, especially in those undergoing atresia (Hurst *et al.*, 2006). However, moderate apoptosis rates may not necessarily be related to follicle death, but triggered by rapid GC proliferation in relatively hypoxic conditions (Thompson *et al.*, 2015). Caspase-3 activity and apoptotic features have also been observed in oocytes of early-stage follicles (Escobar *et al.*, 2008; Albamonte *et al.*, 2019), albeit to a lesser extent.

Oocyte apoptosis has been shown to be a physiological process of cell turnover in fetal ovaries (Vaskivuo *et al.*, 2001; Sadeu *et al.*, 2006), causing an overall loss of 85% of the original pool of oogonia at birth

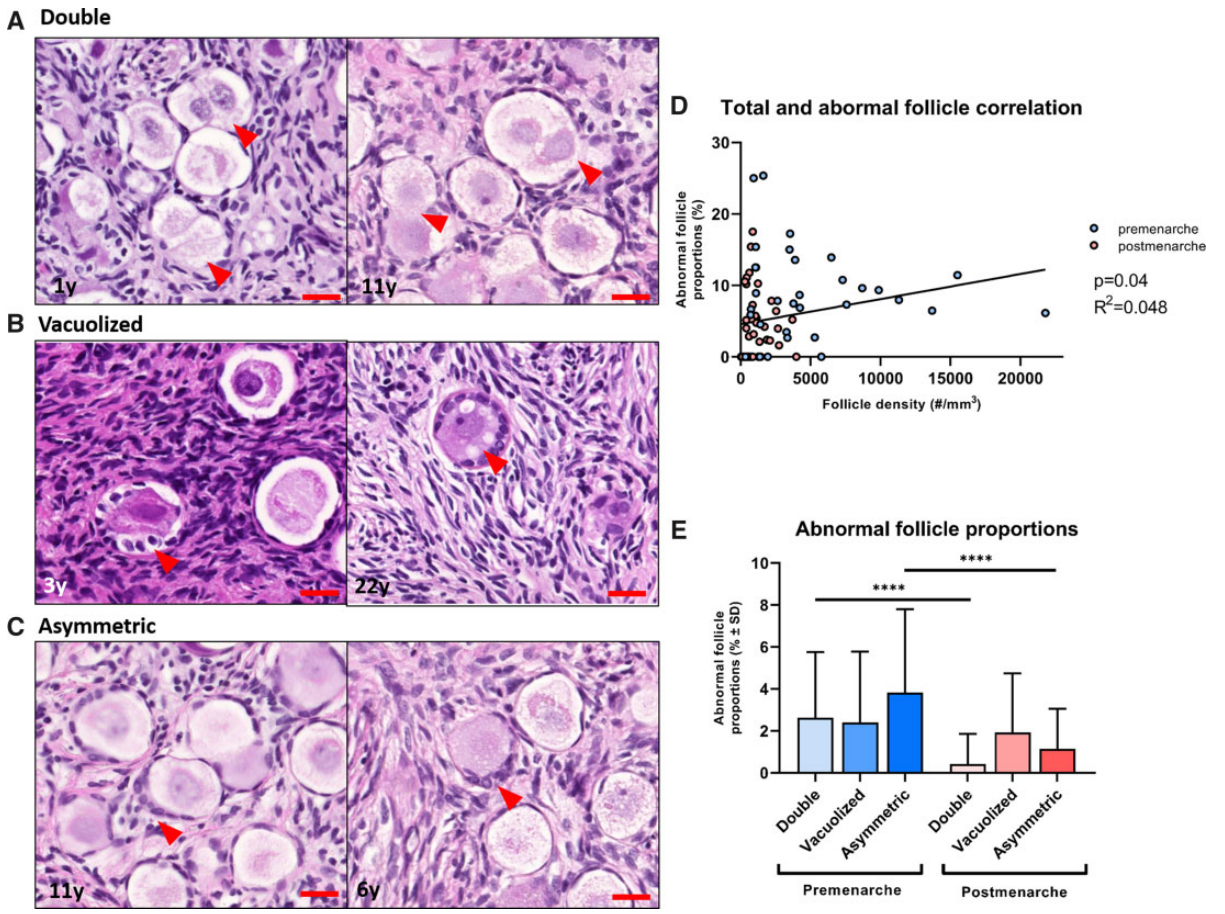

Figure 4. Analysis of morphological abnormalities in follicles and their relation with age. Hematoxylin and eosin staining showing abnormal follicles (**A**) containing two oocytes, or two nuclei in the same oocyte (red arrows). (**B**) Evidence of vacuoles in granulosa cells (GCs) or the oocyte cytoplasm. (**C**) Asymmetric GCs with growth in multiple layers in one spot (red arrows). Scale bar: 20 µm. (**D**) Correlation between follicle density (#/mm^3) and abnormal follicle proportions (%), showing a direct link between these two. (**E**) Comparison of abnormal follicle subtypes (double, vacuolized and asymmetric) in premenarchal and postmenarchal patients. ***$P < 0.0001$. CHT, chemotherapy.

(Albamonte *et al.*, 2008). Evidence of increasing apoptosis kinetics during puberty, along with an increase in follicle growth, has been detected in small series of patients (Albamonte *et al.*, 2013). Our series did not, however, demonstrate changes in either caspase-3 expression or atretic follicle rates with the onset of menarche, which were actually lower after puberty. This indicates that apoptosis is not a phenomenon that depends on the ovarian reserve or kinetic changes with pubertal development but occurs continuously from birth to reproductive age.

The majority of investigations are related to non-physiological contexts, such as response to insults capable of causing DNA damage, including CHT and radiotherapy (Winship *et al.*, 2018; Spears *et al.*, 2019). A recent publication by Albamonte *et al.* (2019) suggests that extragonadal cancer may be responsible for activating apoptosis in the ovarian reserve of adolescents, irrespective of previous CHT. Our data showed higher apoptosis rates only in premenarchal subjects with previous CHT, confirming that this pathway is activated by drugs known to induce DNA damage in oocytes, such as alkylating agents, but not by cancer itself.

According to morphological and ultrastructural analyses, autophagic activity in the follicle pool also appears to be a continuous process, involving around 20% of follicles at all ages. These findings indicate that autophagy plays a crucial role in the human ovarian reserve, as already seen in a number of studies in mice (Gawriluk *et al.*, 2011; Song *et al.*, 2015). Cell renewal is of major importance in tissue with slow-replicating or non-replicating cells, like oocytes in the ovary, which require this ability to survive in a quiescent state from birth until their recruitment for growth at reproductive age. The present study shows increased autophagic activity in follicles of young women diagnosed with a malignancy, suggesting that it is possible for major stressors such as cancer to interact with the ovarian follicle pool. Autophagy may also be induced by various disruptors, including starvation, metabolic changes, inflammation and oxidative stress (Escobar *et al.*, 2008). Oxidative stress is known to be increased in the event of cancer

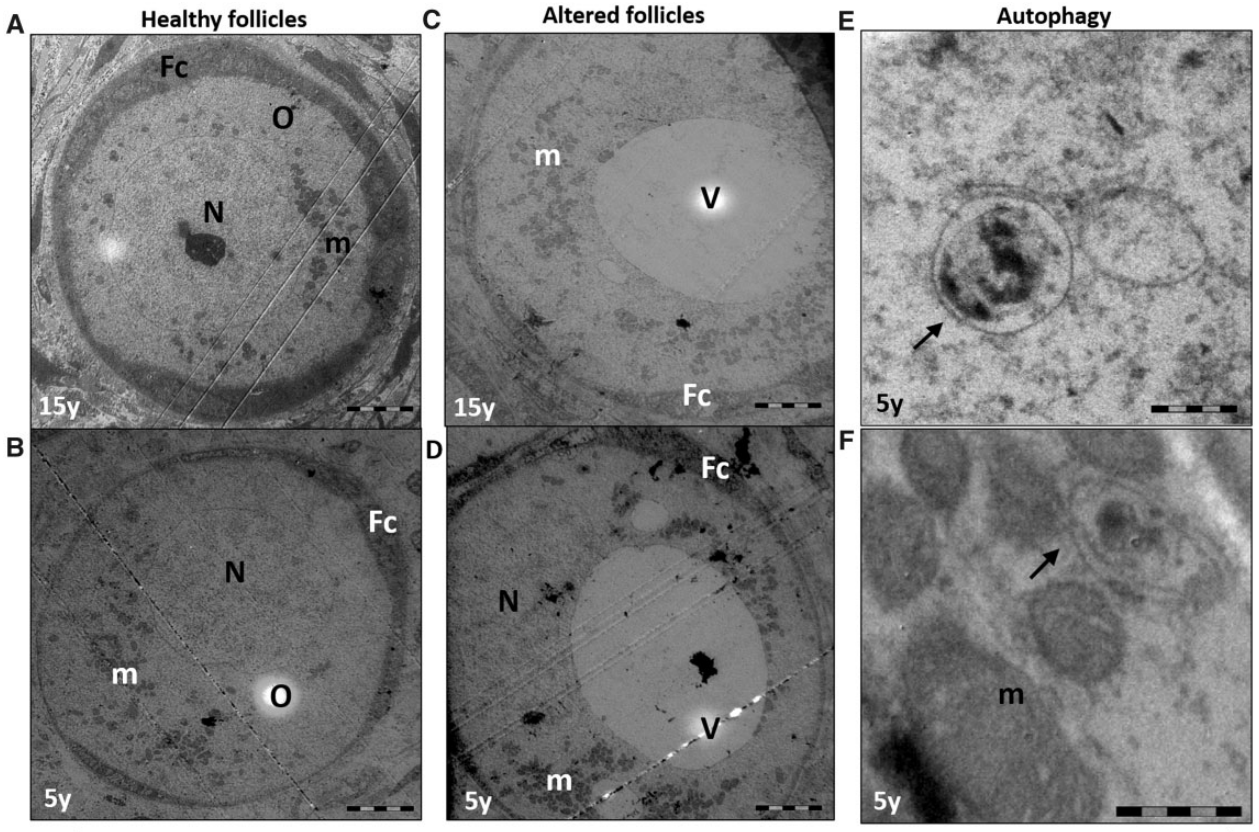

G

	Premenarche (2)	Postmenarche (7)	Postmenarche + previous CHT (4)	
Number of analyzed follicles	30 *	53	33	
Healthy follicles (%)	16/30 (53%)	38/53 (71%)	28/33 (85%)	*ns* **
Autophagic follicle death (%)	8/30 (26%)	0/53	0/33	*ns* **
Autophagic activity (%)	20/30 (66%)	7/53 (13%)	2/33 (6%)	*ns* **

ns: not significant
*Follicles found only in ovarian fragments from one premenarchal patient
** Statistical analyses were done only between 'postmenarche' and 'postmenarche with CHT prior to OTC'

Figure 5. Transmission electron microscopy analysis of follicle morphology and accumulation of autophagosomes. Transmission electron microscopy analyses: (**A** and **B**) Healthy preantral follicles in subjects aged 15 and 5 years (y), (**C** and **D**) abnormal preantral follicles in subjects aged 15 and 5 years and (**E** and **F**) autophagosomes in the oocyte cytoplasm in subjects aged 5 years. (**G**) Comparisons of healthy follicle, autophagic follicle death and autophagic activity rates in premenarchal (n = 1), postmenarchal (n = 7) and postmenarchal subjects undergoing CHT prior to ovarian tissue cryopreservation (n = 4). Bar (A–D): 5 µm; (E and F): 0.5 µm. CHT, chemotherapy; Fc, follicular cell; m, mitochondria; N, nucleus; O, oocyte; V, vacuole; arrow, autophagosomes.

above all, and also potentially co-responsible for its onset and progression (Senthil *et al.*, 2004; Torresano *et al.*, 2020). Further investigations are needed to determine whether autophagy activation plays a protective or detrimental role in the ovarian reserve, since it is not related to elevated apoptosis rates.

Moreover, in considering sizable evidence of autophagy causing follicle death, we found that this phenomenon is age dependent and occurs around 10 times more in premenarchal subjects. This was corroborated by TEM analysis, which was not only found to be more sensitive at detecting autophagy in follicles (Escobar *et al.*, 2008) but also confirmed autophagic follicle death only in the premenarchal group. Follicle death owing to autophagy may be the key mechanism responsible for ovarian pool decline in the first few years after birth (Anderson *et al.*, 2014; Philippart *et al.*, 2021). Autophagy modulation toward cell renewal or death appears to govern selective depletion of these abnormal follicles that are not capable of further development and growth in adult life, as also observed after xenotransplantation of prepubertal ovarian tissue (Luyckx *et al.*, 2013;

Masciangelo et al., 2020). Indeed, according to our results, abnormal follicles decrease in number and proportion not only with advancing age but also after CHT in premenarchal patients. This may point to the intrinsically fragile nature of these follicles, which lack the necessary morphological and functional features to recover from cell damage, survive and develop. Further studies should be conducted to elucidate these aspects.

The impact of specific chemotherapeutic protocols on the ovarian reserve could not be investigated, since the group of patients who had received CHT prior to OTC was very heterogeneous in terms of type of CHT and interval to cryopreservation. Nevertheless, since the debate on the effects of CHT on the ovarian follicle pool is still ongoing (Dolmans et al., 2021b), we could not exclude this group *a priori* when exploring ovarian follicle kinetics and death mechanisms. Our analyses on follicle kinetics in premenarchal and postmenarchal subjects evidenced a different impact of prior CHT in the two study groups. An increase in apoptosis rates and selective decrease in abnormal follicles were observed in premenarchal subjects who had undergone CHT, but no signs of accelerated follicle activation were noted in this group. On the other hand, a significant upturn in growing follicles was detected in postmenarchal patients who had had CHT, but there was no difference in follicle ultrastructure or any of the follicle death pathways. Mechanisms of both accelerated follicle activation and increased follicle death have been described in the literature as a consequence of CHT. Some authors consider the impact of CHT on the follicle pool to be an apoptosis trigger (Luan et al., 2019; Nguyen et al., 2021), while others speculate on the ability of certain chemotherapeutic agents to induce accelerated follicle activation (Kalich-Philosoph et al., 2013; Goldman et al., 2017; Shai et al., 2021).

When looking at parameter estimates that failed to show significant differences, caution is required since dividing patients into subgroups of interest reduces the sample size and hence the likelihood of identifying existing differences between them. Looking at what the present article has demonstrated, this was the first time that apoptosis and autophagy signaling pathways have been associated with patient age. Our findings, showing different follicle behavior after CHT depending on age, suggest that these treatments may trigger one response or the other depending on the size and quality of the ovarian reserve. Quiescent follicles, and more specifically those that are morphologically abnormal, appear to die after CHT as a result of apoptosis in premenarchal ovaries but look to be activated for growth in postmenarchal subjects.

The present study provides a picture of the ovarian follicle pool in a large series of patients of different ages and with disparate clinical history, but caution should be exercised in drawing conclusions about autophagy pathway modulations. Although our analyses were able show accumulation of autophagosomes, which is suggestive of cell death, further investigations are needed to shed light on the actual purpose of autophagy activation, since it can promote both cell death and survival.

In conclusion, follicle pool depletion throughout the first decades of a woman's life is a complex event in which signaling pathways play different roles according to age, and the size and quality of the ovarian reserve. Follicle atresia not only reduces follicle numbers over time but also appears to selectively reject those with morphological alterations. Among follicle death pathways, autophagy is likely crucial to ovarian reserve depletion before menarche, probably contributing to the elimination of abnormal and damaged follicles. In the event of exogenous damage, as seen after CHT, these cell death pathways also seem to depend on age and ovarian reserve size, triggering an increase in follicle apoptosis in premenarchal subjects and acceleration of follicle activation in postmenarchal women.

Supplementary data

Supplementary data are available at *Human Reproduction* online.

Data availability

The data underlying this article will be shared on reasonable request to the corresponding author.

Acknowledgements

The authors thank Mira Hryniuk, B.A., for reviewing the English language of the article and Dolores Gonzalez and Sarah Storder for their technical assistance.

Authors' roles

L.C. and A.Ca. designed the study. L.C. and A.Ce. performed the histological analyses and extracted the corresponding data. A.Ca. performed the TEM analyses and extracted corresponding the data. L.C. did the statistical analyses and wrote the article. J.D. and MM.D revised the article.

Funding

This study was supported by grants from the Fonds National de la Recherche Scientifique de Belgique (F.R.S.-FNRS/FRIA FC29657 awarded to L.Ca., CDR J.0063.20 and grant 5/4/150/5 awarded to M.M.D.), grants from the Fondation contre le Cancer (grant 2018-042 awarded to A.Ca.), the Fondazione Comunitaria del Varesotto and Provincia di Varese ('Amalia Griffini' Fellowship in Gynecology and Obstetrics awarded to A.Ce.), Fonds Spéciaux de Recherche, Fondation St Luc and donations from the Ferrero family.

Conflict of interest

The authors have nothing to disclose.

References

Albamonte MS, Willis MA, Albamonte MI, Jensen F, Espinosa MB, Vitullo AD. The developing human ovary: immunohistochemical analysis of germ-cell-specific VASA protein, BCL-2/BAX expression balance and apoptosis. *Hum Reprod* 2008;**23**:1895–1901.

Albamonte MI, Albamonte MS, Stella I, Zuccardi L, Vitullo AD. The infant and pubertal human ovary: Balbiani's body-associated VASA expression, immunohistochemical detection of apoptosis-related

BCL2 and BAX proteins, and DNA fragmentation. *Hum Reprod* 2013;**28**:698–706.

Albamonte MI, Albamonte MS, Bou-Khair RM, Zuccardi L, Vitullo AD. The ovarian germinal reserve and apoptosis-related proteins in the infant and adolescent human ovary. *J Ovarian Res* 2019;**12**: 22.

Amorim CA, Donnez J, Dehoux JP, Scalercio SR, Squifflet J, Dolmans MM. Long-term follow-up of vitrified and autografted baboon (Papio anubis) ovarian tissue. *Hum Reprod* 2019;**34**:323–334.

Anderson RA, McLaughlin M, Wallace WH, Albertini DF, Telfer EE. The immature human ovary shows loss of abnormal follicles and increasing follicle developmental competence through childhood and adolescence. *Hum Reprod* 2014;**29**:97–106.

BAKER TG. A quantitative and cytological study of germ cells in human ovaries. *Proc R Soc Lond B: Biol Sci* 1963;**158**:417–433.

Cacciottola L, Courtoy GE, Nguyen TYT, Hossay C, Donnez J, Dolmans MM. Adipose tissue-derived stem cells protect the primordial follicle pool from both direct follicle death and abnormal activation after ovarian tissue transplantation. *J Assist Reprod Genet* 2021;**38**:151–161.

Camboni A, Martinez-Madrid B, Dolmans MM, Amorim CA, Nottola SA, Donnez J, Van Langendonckt A. Preservation of fertility in young cancer patients: contribution of transmission electron microscopy. *Reprod Biomed Online* 2008;**17**:136–150.

Choi J, Jo M, Lee E, Choi D. Induction of apoptotic cell death via accumulation of autophagosomes in rat granulosa cells. *Fertil Steril* 2011;**95**:1482–1486.

Dolmans MM, Martinez-Madrid B, Gadisseux E, Guiot Y, Yuan WY, Torre A, Camboni A, Van Langendonckt A, Donnez J. Short-term transplantation of isolated human ovarian follicles and cortical tissue into nude mice. *Reproduction* 2007;**134**:253–262.

Dolmans MM, Donnez J, Cacciottola L. Fertility preservation: the challenge of freezing and transplanting ovarian tissue. *Trends Mol Med* 2021a;**27**:777–791.

Dolmans MM, Donnez J. Fertility preservation in women for medical and social reasons: oocytes versus ovarian tissue. *Best Pract Res Clin Obstet Gynaecol* 2021;**70**:63–80.

Dolmans MM, von Wolff M, Poirot C, Diaz-Garcia C, Cacciottola L, Boissel N, Liebenthron J, Pellicer A, Donnez J, Andersen CY. Transplantation of cryopreserved ovarian tissue in a series of 285 women: a review of five leading European centers. *Fertil Steril* 2021b;**115**:1102–1115.

Duerrschmidt N, Zabirnyk O, Nowicki M, Ricken A, Hmeidan FA, Blumenauer V, Borlak J, Spanel-Borowski K. Lectin-like oxidized low-density lipoprotein receptor-1-mediated autophagy in human granulosa cells as an alternative of programmed cell death. *Endocrinology* 2006;**147**:3851–3860.

Ellnati E, Zielinska AP, McCarthy A, Kubikova N, Maciulyte V, Mahadevaiah S, Sangrithi MN, Ojarikre O, Wells D, Niakan KK et al The BCL-2 pathway preserves mammalian genome integrity by eliminating recombination-defective oocytes. *Nat Commun* 2020;**11**:2598.

Escobar ML, Echeverría OM, Ortíz R, Vázquez-Nin GH. Combined apoptosis and autophagy, the process that eliminates the oocytes of atretic follicles in immature rats. *Apoptosis* 2008;**13**:1253–1266.

Escobar ML, Echeverria OM, Palacios-Martínez S, Juárez-Chavero S, Sánchez-Sánchez L, Vázquez-Nin GH. Beclin 1 interacts with active Caspase-3 and Bax in oocytes from atretic follicles in the rat ovary. *J Histochem Cytochem* 2019;**67**:873–889.

Gawriluk TR, Hale AN, Flaws JA, Dillon CP, Green DR, Rucker EB 3rd. Autophagy is a cell survival program for female germ cells in the murine ovary. *Reproduction* 2011;**141**:759–765. Jun

Goldman KN, Chenette D, Arju R, Duncan FE, Keefe DL, Grifo JA, Schneider RJ. mTORC1/2 inhibition preserves ovarian function and fertility during genotoxic chemotherapy. *Proc Natl Acad Sci U S A* 2017;**114**:3186–3191.

Gougeon A, Chainy GB. Morphometric studies of small follicles in ovaries of women at different ages. *J Reprod Fertil* 1987;**81**: 433–442.

Gougeon A, Ecochard R, Thalabard JC. Age-related changes of the population of human ovarian follicles: increase in the disappearance rate of non-growing and early-growing follicles in aging women. *Biol Reprod* 1994;**50**:653–663.

Gougeon A. Regulation of ovarian follicular development in primates: facts and hypotheses. *Endocr Rev* 1996;**17**:121–155.

Grillo F, Bruzzone M, Pigozzi S, Prosapio S, Migliora P, Fiocca R, Mastracci L. Immunohistochemistry on old archival paraffin blocks: is there an expiry date? *J Clin Pathol* 2017;Nov**70**:988–993.

Hartley PS, Bayne RA, Robinson LL, Fulton N, Anderson RA. Developmental changes in expression of myeloid cell leukemia-1 in human germ cells during oogenesis and early folliculogenesis. *J Clin Endocrinol Metab* 2002;**87**:3417–3427.

Hurst PR, Mora JM, Fenwick MA. Caspase-3, TUNEL and ultrastructural studies of small follicles in adult human ovarian biopsies. *Hum Reprod* 2006;**21**:1974–1980.

Kalich-Philosoph L, Roness H, Carmely A, Fishel-Bartal M, Ligumsky H, Paglin S, Wolf I, Kanety H, Sredni B, Meirow D. Cyclophosphamide triggers follicle activation and "burnout"; AS101 prevents follicle loss and preserves fertility. *Sci Transl Med* 2013;**5**: 185ra62.

Kitajima M, Dolmans MM, Donnez O, Masuzaki H, Soares M, Donnez J. Enhanced follicular recruitment and atresia in cortex derived from ovaries with endometriomas. *Fertil Steril* 2014;**101**: 1031–1037.

Klionsky DJ, Abdel-Aziz AK, Abdelfatah S, Abdellatif M, Abdoli A, Abel S, Abeliovich H, Abildgaard MH, Abudu YP, Acevedo-Arozena A, *et al*. Guidelines for the Use and Interpretation of Assays for Monitoring Autophagy (4th edition). *Autophagy*. 2021; **17**:1–382.

Luan Y, Edmonds ME, Woodruff TK, Kim S. Inhibitors of apoptosis protect the ovarian reserve from cyclophosphamide. *J Endocrinol* 2019;**240**:243–256.

Luyckx V, Scalercio S, Jadoul P, Amorim CA, Soares M, Donnez J, Dolmans MM. Evaluation of cryopreserved ovarian tissue from prepubertal patients after long-term xenografting and exogenous stimulation. *Fertil Steril* 2013;**100**:1350–1357.

Maidarti M, Anderson RA, Telfer EE. Crosstalk between PTEN/PI3K/Akt signalling and DNA damage in the oocyte: implications for primordial follicle activation, oocyte quality and ageing. *Cells* 2020;**9**:200.

Mamsen LS, Charkiewicz K, Anderson RA, Telfer EE, McLaughlin M, Kelsey TW, Kristensen SG, Gook DA, Ernst E, Andersen CY. Characterization of follicles in girls and young women with Turner

syndrome who underwent ovarian tissue cryopreservation. *Fertil Steril* 2019;**111**:1217–1225.e3.

Martinet W, Timmermans JP, De Meyer GR. Methods to assess autophagy in situ–transmission electron microscopy versus immunohistochemistry. *Methods Enzymol* 2014;**543**:89–114.

Masciangelo R, Chiti MC, Philippart C, Amorim CA, Donnez J, Camboni A, Dolmans MM. Follicle populations and vascularization in ovarian tissue of pediatric patients before and after long-term grafting. *Fertil Steril* 2020;**114**:1330–1338.

Nguyen QN, Zerafa N, Findlay JK, Hickey M, Hutt KJ. DNA repair in primordial follicle oocytes following cisplatin treatment. *J Assist Reprod Genet* 2021;**38**:1405–1417.

Nottola SA, Heyn R, Camboni A, Correr S, Macchiarelli G. Ultrastructural characteristics of human granulosa cells in a coculture system for in vitro fertilization. *Microsc Res Tech* 2006;**69**: 508–516.

Peters AE, Caban SJ, McLaughlin EA, Roman SD, Bromfield EG, Nixon B, Sutherland JM. The impact of aging on macroautophagy in the pre-ovulatory mouse oocyte. *Front Cell Dev Biol* 2021;**9**: 691826.

Philippart C, Masciangelo R, Camboni A, Donnez J, Dolmans MM. Basal lamina characterization in frozen-thawed and long-term grafted human prepubertal ovarian tissue. *Reprod Biomed Online* 2021;**42**:859–869.

Rubinsztein DC, Mariño G, Kroemer G. Autophagy and aging. *Cell* 2011;**146**:682–695.

Sadeu JC, Cortvrindt R, Ron-El R, Kasterstein E, Smitz J. Morphological and ultrastructural evaluation of cultured frozen-thawed human fetal ovarian tissue. *Fertil Steril* 2006;**85**:1130–1141.

Sanchez AM, Papaleo E, Corti L, Santambrogio P, Levi S, Viganò P, Candiani M, Panina-Bordignon P. Iron availability is increased in individual human ovarian follicles in close proximity to an endometrioma compared with distal ones. *Hum Reprod* 2014;**29**:577–583.

Senthil K, Aranganathan S, Nalini N. Evidence of oxidative stress in the circulation of ovarian cancer patients. *Clin Chim Acta* 2004;**339**: 27–32.

Shai D, Aviel-Ronen S, Spector I, Raanani H, Shapira M, Gat I, Roness H, Meirow D. Ovaries of patients recently treated with alkylating agent chemotherapy indicate the presence of acute follicle activation, elucidating its role among other proposed mechanisms of follicle loss. *Fertil Steril* 2021;**115**:1239–1249.

Song ZH, Yu HY, Wang P, Mao GK, Liu WX, Li MN, Wang HN, Shang YL, Liu C, Xu ZL *et al.* Germ cell-specific Atg7 knockout results in primary ovarian insufficiency in female mice. *Cell Death Dis* 2015;**6**:e1589. Jan 15

Spears N, Lopes F, Stefansdottir A, Rossi V, De Felici M, Anderson RA, Klinger FG. Ovarian damage from chemotherapy and current approaches to its protection. *Hum Reprod Update* 2019;**25**: 673–693.

Thompson JG, Brown HM, Kind KL, Russel DL. The ovarian antral follicle: living on the edge of hypoxia or not? *Biol Reprod* 2015;**92**: 153.

Tilly JL. Commuting the death sentence: how oocytes strive to survive. *Nat Rev Mol Cell Biol* 2001;**2**:838–848.

Tiwari M, Prasad S, Tripathi A, Pandey AN, Ali I, Singh AK, Shrivastav TG, Chaube SK. Apoptosis in mammalian oocytes: a review. *Apoptosis* 2015;**20**:1019–1025.

Tiwari M, Tripathi A, Chaube SK. Presence of encircling granulosa cells protects against oxidative stress-induced apoptosis in rat eggs cultured in vitro. *Apoptosis* 2017;**22**:98–107.

Torresano L, Nuevo-Tapioles C, Santacatterina F, Cuezva JM. Metabolic reprogramming and disease progression in cancer patients. *Biochim Biophys Acta Mol Basis Dis* 2020;**1866**:165721.

Vaskivuo TE, Anttonen M, Herva R, Billig H, Dorland M, te Velde ER, Stenbäck F, Heikinheimo M, Tapanainen JS. Survival of human ovarian follicles from fetal to adult life: apoptosis, apoptosis-related proteins, and transcription factor GATA-4. *J Clin Endocrinol Metab* 2001;**86**:3421–3429.

Vaskivuo TE, Tapanainen JS. Apoptosis in the human ovary. *Reprod Biomed Online* 2003;**6**:24–35.

Wallace WH, Kelsey TW. Human ovarian reserve from conception to the menopause. *PLoS One* 2010;**5**:e8772.

Winship AL, Stringer JM, Liew SH, Hutt KJ. The importance of DNA repair for maintaining oocyte quality in response to anti-cancer treatments, environmental toxins and maternal ageing. *Hum Reprod Update* 2018;**24**:119–134.

Yadav AK, Yadav PK, Chaudhary GR, Tiwari M, Gupta A, Sharma A, Pandey AN, Pandey AK, Chaube SK. Autophagy in hypoxic ovary. *Cell Mol Life Sci* 2019;**76**:3311–3322.

Zhou J, Peng X, Mei S. Autophagy in ovarian follicular development and atresia. *Int J Biol Sci* 2019;**15**:726–737.